Supporting Information for *New Journal of Chemistry*

Triplet biradical with double bidentate sites based on *tert*-butyl pyridyl nitroxide as a candidate for strong ferromagnetic couplers

Atsushi Okazawa,*[a] Yutaro Terakado,[b] Takayuki Ishida *[b] and Norimichi Kojima [c]

[a] *Department of Basic Science, Graduate School of Arts and Sciences, The University of Tokyo, Tokyo 153-8902, Japan*
[b] *Department of Engineering Science, The University of Electro-Communications, Tokyo 182-8585, Japan*
[c] *Toyota Physical and Chemical Research Institute, Aichi 480-1192, Japan*

E-mail: cokazawa@mail.ecc.u-tokyo.ac.jp, takayuki.ishida@uec.ac.jp

Contents

Syntheses

All reagents and solvents were obtained from commercial source and used as received without purification.

6,2′-Dibromo-3,4′-bipyridyl (34bpyBr$_2$)

The material was synthesized from 2-bromo-5-pyridylboronic acid and 2-bromo-4-iodopyridine by the Suzuki–Miyaura coupling reaction, where the synthetic procedure is slightly modified based on the method of the literature.[1] A mixture of 2-bromo-5-pyridylboronic acid (15.5 g; 77.0 mmol), 2-bromo-4-iodopyridine (21.9 g, 77.0 mmol), and $Pd(PPh_3)_4$ (1.40 g, 1.57 mol %) in deaerated THF (200 mL) was heated at 50 °C for 1 h, and then Na_2CO_3 (20.4 g, 192 mmol) in deaerated distilled water (100 mL) was added to the solution. The mixture was heated at 50 °C for 12 h. The THF solvent was removed from the reaction mixture. After the residue was dissolved in dichloromethane, the organic layer was washed with water, dried over anhydrous Na_2SO_4, filtered, and evaporated. The crude product was washed with dichloromethane on a filter. A colorless powdery product was obtained in 41% yield. (9.80 g, 31.2 mmol). Mp 195.2–197.0 °C. ^{1}H NMR ($CDCl_3$, 500 MHz) δ 8.62 (2-py, dd, *J* = 2.6, 0.7 Hz, 1H), 8.48 (6′-py, dd, *J* = 5.2, 0.6 Hz, 1H), 7.76 (4-py, dd, *J* = 8.3, 2.6 Hz, 1H), 7.68 (3′-py, dd, *J* = 1.6, 0.6 Hz, 1H), 7.64 (5-py, dd, *J* = 8.3, 0.7 Hz, 1H), 7.44 (5′-py, dd, *J* = 5.2, 1.6 Hz, 1H). *Note that the literature[1] shows a very low melting point (< 50 °C) and no ^{1}H-^{1}H coupling between the 3- and 4-positions on the pyridine ring (6-bromopyridine-4-yl side) in the ^{1}H NMR spectrum.*

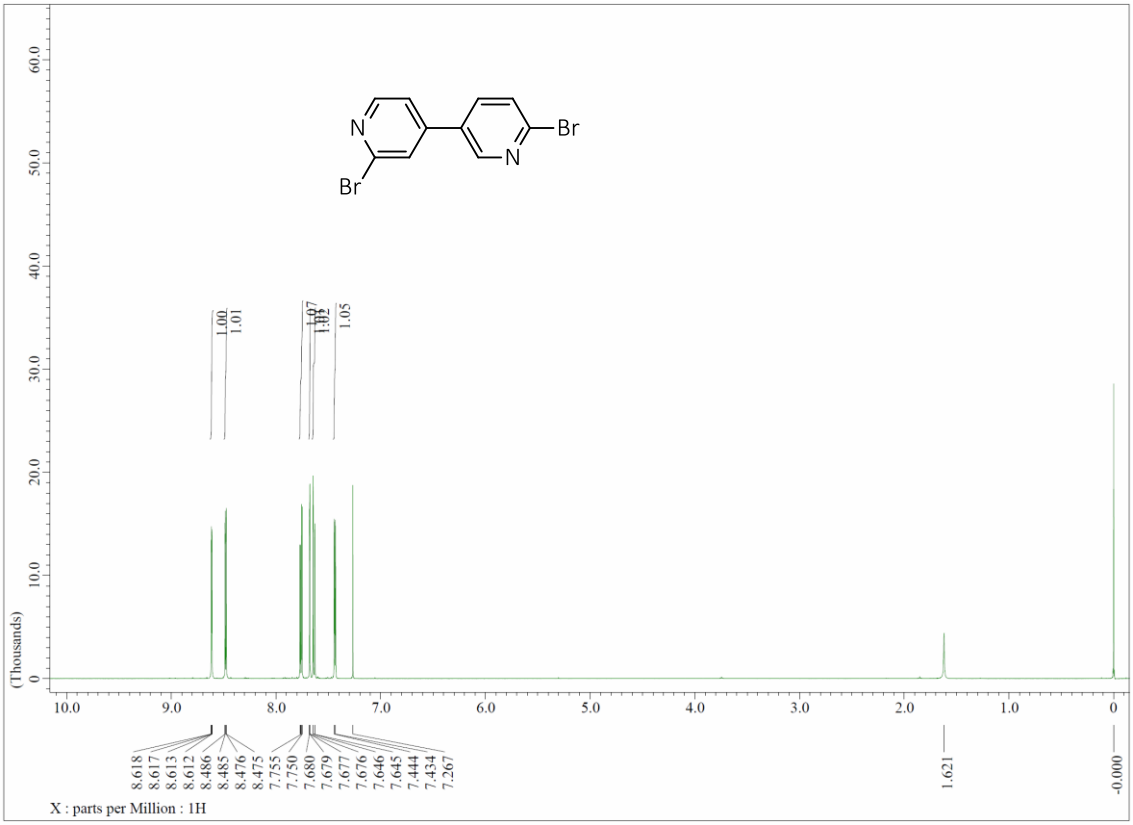

Figure S1 ^{1}H NMR spectra of 34bpyBr$_2$ ($CDCl_3$, 500 MHz).

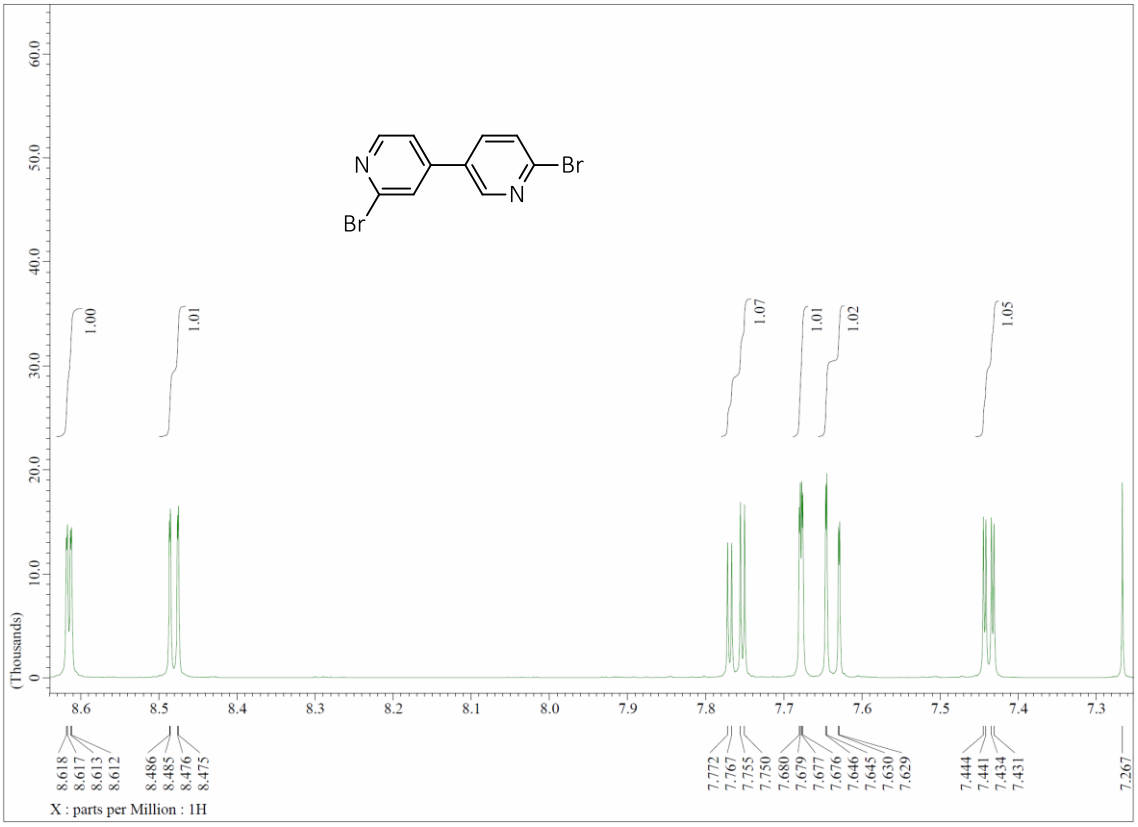

Figure S2 Expanded view of ^{1}H NMR spectra of 34bpyBr$_2$ in a low-field region.

6,2′-Bis(*N*-*tert*-butylhydroxylamino)-3,4′-bipyridyl (34bpybNOH)

A hexane solution (20.2 mL, 1.63 mol/L) of *n*-BuLi (33.0 mmol) was added dropwise to a dehydrated THF solution (450 mL) containing 34bpyBr$_2$ (4.71 g, 15.0 mmol) by a syringe at –98 °C under nitrogen atmosphere. The mixture was stirred at –98 °C for 1 h. Subsequently, a dehydrated THF solution (50 mL) involving 2-methyl-2-nitrosopropane (192 mg, 2.20 mmol) was added from a dropping funnel at –98 °C for about 30 min. The mixture was gradually warmed up to around –40 °C, quenched with aqueous ascorbic acid (ca. 1 g, 10 mL) for preventing air oxidation of the title hydroxylamine. After the solvents were removed by a rotary evaporator, the products were separated on a silica-gel chromatography eluted with 5/1 to 1/1 chloroform–ethyl-acetate solvents. Concentration of the eluent under reduced pressure gave a crude product. Precipitation from ether/hexane, suction filtration, and drying *in vacuo* afforded 34bpybNOH as pale cream powder (1.26 g, 3.80 mmol, yield 25%). Mp > 127 °C (dec.). ^{1}H NMR (DMSO-d_6, 500 MHz) δ 9.08 (-NOH, s, 1H), 8.87 (-NOH, s, 1H), 8.51 (2-py, dd, J = 2.6, 0.5 Hz, 1H), 8.20 (6′-py, dd, J = 5.2, 0.5 Hz, 1H), 7.93 (4-py, dd, J = 8.8, 2.6 Hz, 1H), 7.41 (3′-py, dd, J = 1.6, 0.5 Hz, 1H), 7.26 (5-py, dd, J = 8.8, 0.5 Hz, 1H), 7.14 (5′-py, dd, J = 5.2, 1.6 Hz, 1H), 1.40 (^{t}Bu, s, 9H), 1.35 (^{t}Bu, s, 9H). ^{13}C NMR (DMSO-d_6, 126 MHz) δ 164.7, 164.1, 146.9, 145.6, 144.2, 135.1, 125.1, 113.2, 112.6, 109.4, 60.9, 60.7, 27.4, 27.4. IR (ATR) 809, 826, 1196, 1218, 1358, 1407, 1462, 1593, 2975, 3333 cm^{-1}. Anal. Calcd for $C_{18}H_{26}N_4O_2$: C, 65.43; H, 7.93; N, 16.96. Found: C, 65.57; H, 8.07; N, 17.11%.

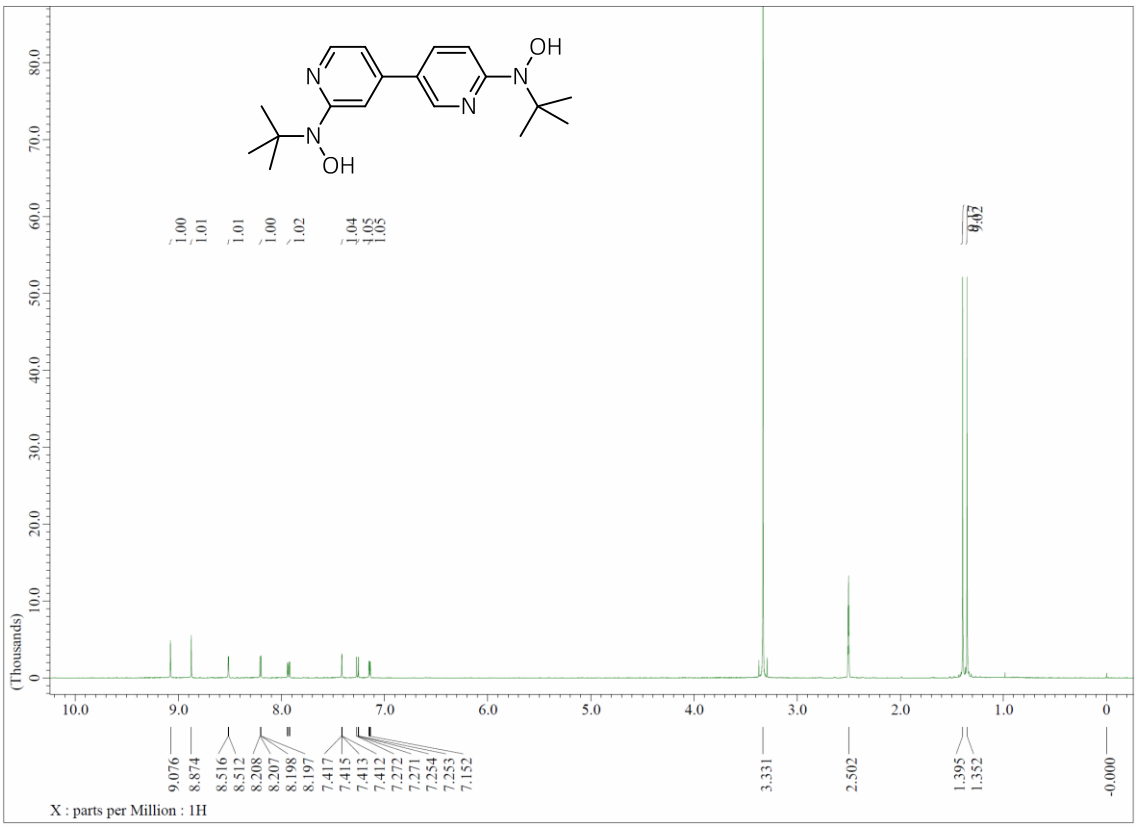

Figure S3 ^{1}H NMR spectra of 34bpybNOH (DMSO-d_6, 500 MHz).

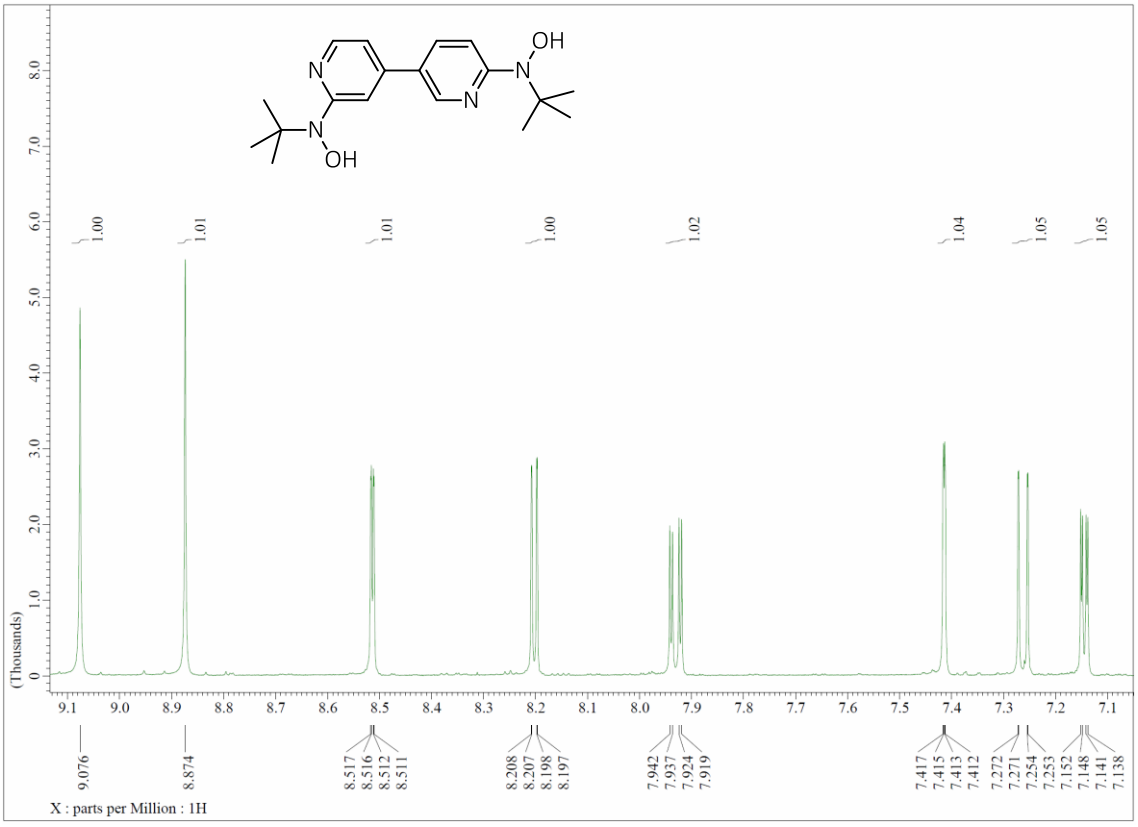

Figure S4 Expanded view of ^{1}H NMR spectra of 34bpybNOH in a low-field region.

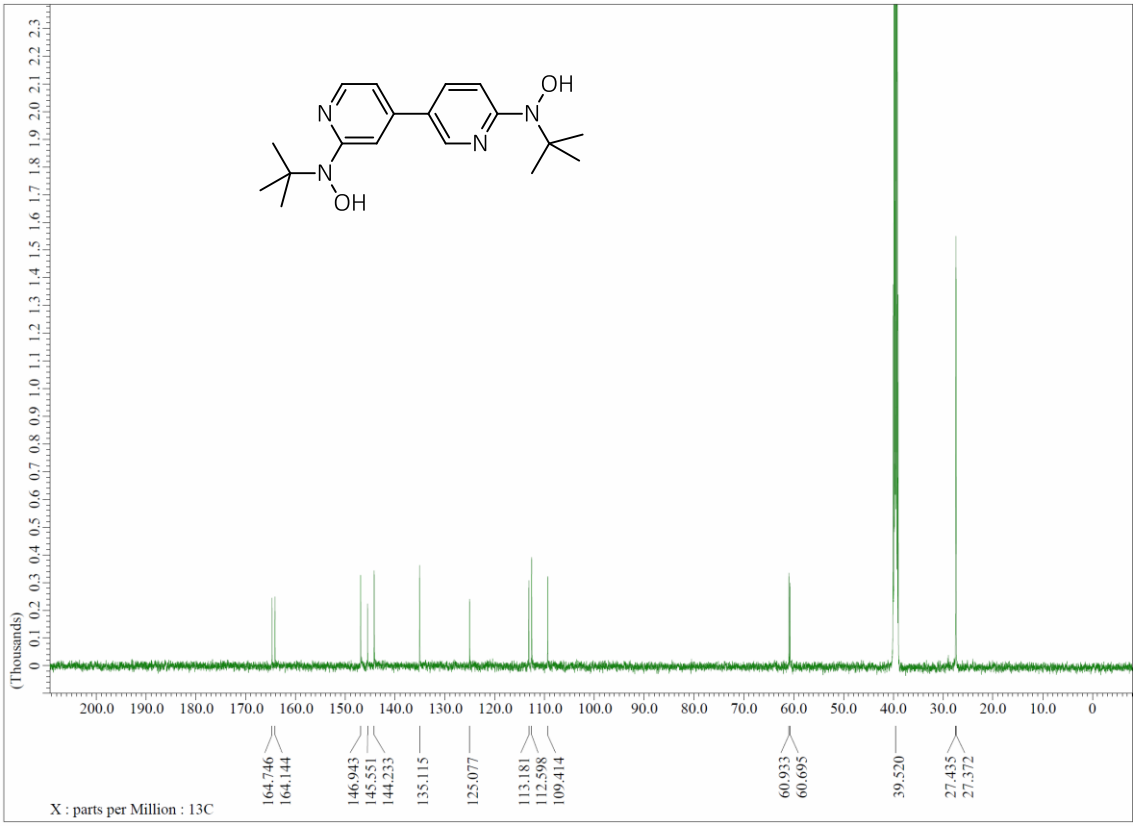

Figure S5 ^{13}C NMR spectra of 34bpybNOH (DMSO-d_6, 126 MHz).

3,4′-Bipyridyl-6,2′-diyl bis(*tert*-butyl nitroxide)

Freshly prepared Ag_2O (3.39 g, 14.6 mmol, 2.0 eq per NOH group) was added to a dichloromethane solution (50 mL) containing 34bpybNOH (1.21 g, 3.66 mmol), and then the mixture was stirred at room temperature for 1 h. Filtration followed by concentration under reduced pressure gave a crude solid product. The target material was purified by passing a short column (silica gel; chloroform as an eluent). Recrystallization from hexane afforded good crystalline solids (0.820 g, 2.50 mmol, yield 68%) for X-ray diffraction study. Mp 90.5–91.5 °C (dec.). IR (ATR) 534, 822, 1187, 1246, 1360, 1394, 1457, 1589, 2932, 2974 cm^{-1}. Anal. Calcd for $C_{18}H_{26}N_4O_2$: C, 65.83; H, 7.37; N, 17.06. Found: C, 65.84; H, 7.50; N, 17.14%.

DFT calculations

Density functional theory (DFT) calculations were performed on the Gaussian09 program[2] with unrestricted hybrid functional DFT methods, UB3LYP, with the Becke exchange functional[3] and the Lee−Yang−Parr correlation functional.[4] The 6−31G(d,p) basis set was chosen. The convergence criterion for the energy was set at 10^{-9} a.u. The SCF energies of the singlet states were obtained according to the broken symmetry (BS) method.[5] The spin density surfaces were drawn at the isovalue of 0.005 e^{-} a.u.$^{-3}$. The SCF energies (and $\langle S^2 \rangle$ values) of the triplet and BS singlet states were converged to E_T = −1069.74741507 ($\langle S^2 \rangle_T$ = 2.0002) and E_{BS} = −1069.74892707 a.u. ($\langle S^2 \rangle_{BS}$ = 0.2205) for the "*para–para*" bipyridine-type biradical, E_T = −1069.74604935 ($\langle S^2 \rangle_T$ = 2.0006) and E_{BS} = −1069.74554341 a.u. ($\langle S^2 \rangle_{BS}$ = 0.1630) for the "*meta–para*" isomer, and E_T = −1069.74759958 ($\langle S^2 \rangle_T$ = 2.0002) and E_{BS} = −1069.74769787 a.u. ($\langle S^2 \rangle_{BS}$ = 0.1831) for the "*meta–meta*" isomer, respectively. The intramolecular exchange couplings (J defined as $H = -2JS_1 \cdot S_2$) were evaluated by Yamaguchi's spin-projected formula[6] to eliminate the effect of the spin contamination from the energy of the BS state, giving as $2J/k_B$ = –537, +174, and –34 K for the "*para–para*", "*meta–para*", and "*meta–meta*" isomers. For the crystal structure of 34bpybNO, the single-point DFT calculations were performed at the UB3LYP/6–31G(d,p) level. The obtained SCF energies of the triplet and BS singlet states were E_T = −1069.51287112 ($\langle S^2 \rangle_T$ = 2.0003) and E_{BS} = −1069.51259174 a.u. ($\langle S^2 \rangle_{BS}$ = 0.1226), respectively.

We also checked the adequacy of the intermolecular interaction which is estimated as $2j/k_B$ = –84(5) K from the magnetic measurement and analysis, using DFT calculations at the UB3LYP/6–31G(d,p) level for the dimeric molecules showing π–π interaction (Figs. S9 and S10) as well as the other possible dimers with an intermolecular magnetic coupling (Fig. S11 and Table S1). We proposed dimeric models removed the outer *tert*-butyl nitroxide groups to extract only an intermolecular exchange coupling. The single-point energies (and $\langle S^2 \rangle$ values) of the triplet and BS singlet states for the π–π dimer were calculated to be E_T = −1564.79578112 ($\langle S^2 \rangle_T$ = 2.0002) and E_{BS} = −1564.79590769 a.u. ($\langle S^2 \rangle_{BS}$ = 0.1393), respectively, affording the intermolecular exchange coupling of $2j/k_B$ = –43 K. Thus, the π–π contact is most likely to be the origin of the intermolecular magnetic coupling.

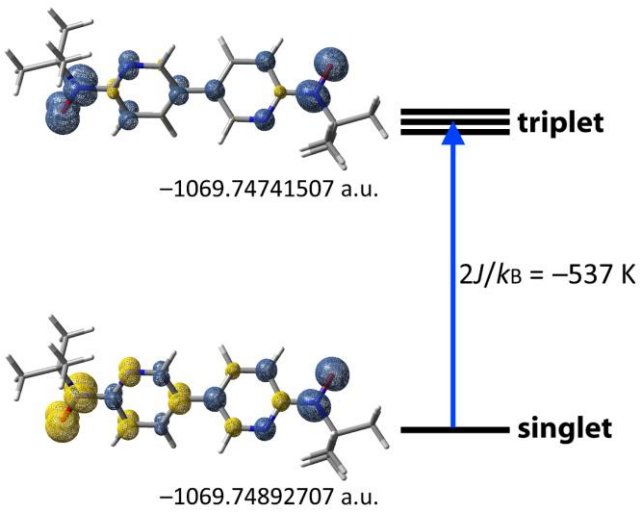

Figure S6 Energy level diagram for triplet and broken-symmetry singlet states in "*para–para*" biradical with the DFT-calculated spin density distributions at the UB3LYP/6–31G(d,p) level. Blue and yellow lobes stand for positive and negative spin densities, respectively. The isovalue is set to 0.005 e^{-} a.u.$^{-3}$.

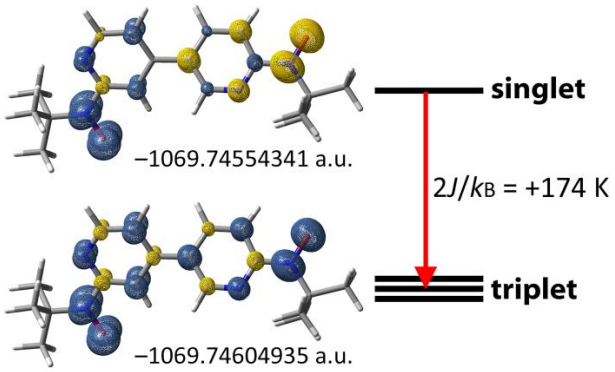

Figure S7 Energy level diagram for triplet and broken-symmetry singlet states in "*meta–para*" biradical (34bpybNO) with the DFT-calculated spin density distributions at the UB3LYP/6–31G(d,p) level. Blue and yellow lobes stand for positive and negative spin densities, respectively. The isovalue is set to 0.005 e^{-} a.u.$^{-3}$.

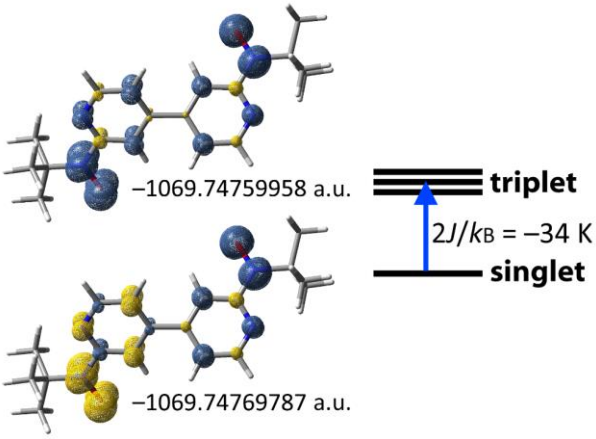

Figure S8 Energy level diagram for triplet and broken-symmetry singlet states in "*meta–meta*" biradical with the DFT-calculated spin density distributions at the UB3LYP/6–31G(d,p) level. Blue and yellow lobes stand for positive and negative spin densities, respectively. The isovalue is set to 0.005 e^{-} a.u.$^{-3}$.

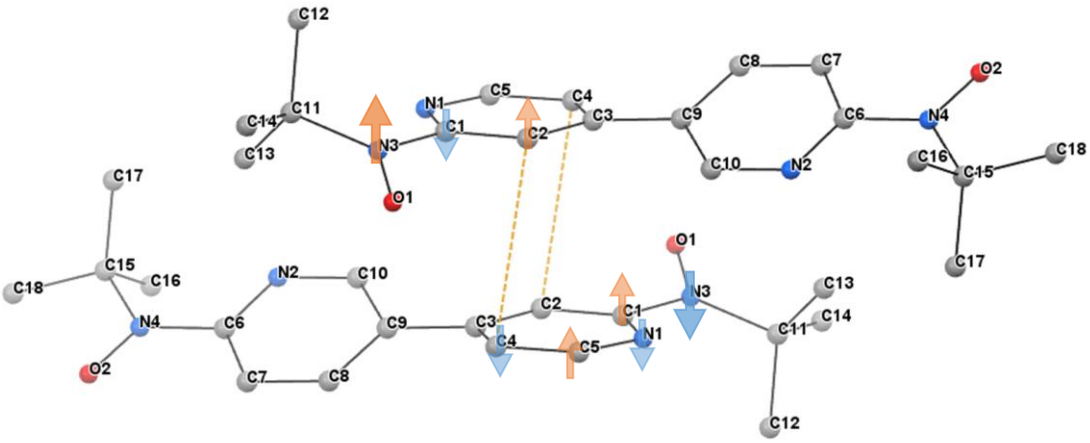

Figure S9 Molecular arrangement in the crystal of 34bpybNO. The hydrogen atoms are omitted for clarity. Dashed lines indicate the interatomic contacts of 3.416(3) Å between the C2 and C4 atoms. The possible spin polarization scheme is shown with arrows.

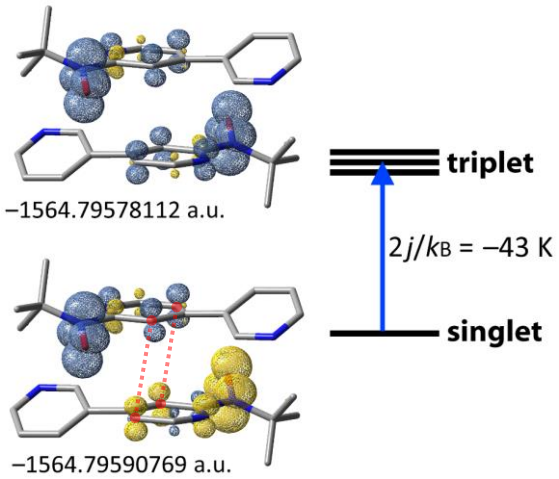

Figure S10 Energy level diagram for triplet and broken-symmetry singlet states in a model for the dimeric molecules showing π–π interaction (see Fig. S9) related to the experimental value ($2j/k_B$ = –84(5) K) of the intermolecular antiferromagnetic coupling, with the DFT-calculated spin density distributions at the UB3LYP/6–31G(d,p) level. Blue and yellow lobes stand for positive and negative spin densities, respectively. The isovalue is set to 0.005 e^- a.u.$^{-3}$. Hydrogen atoms are omitted for clarity.

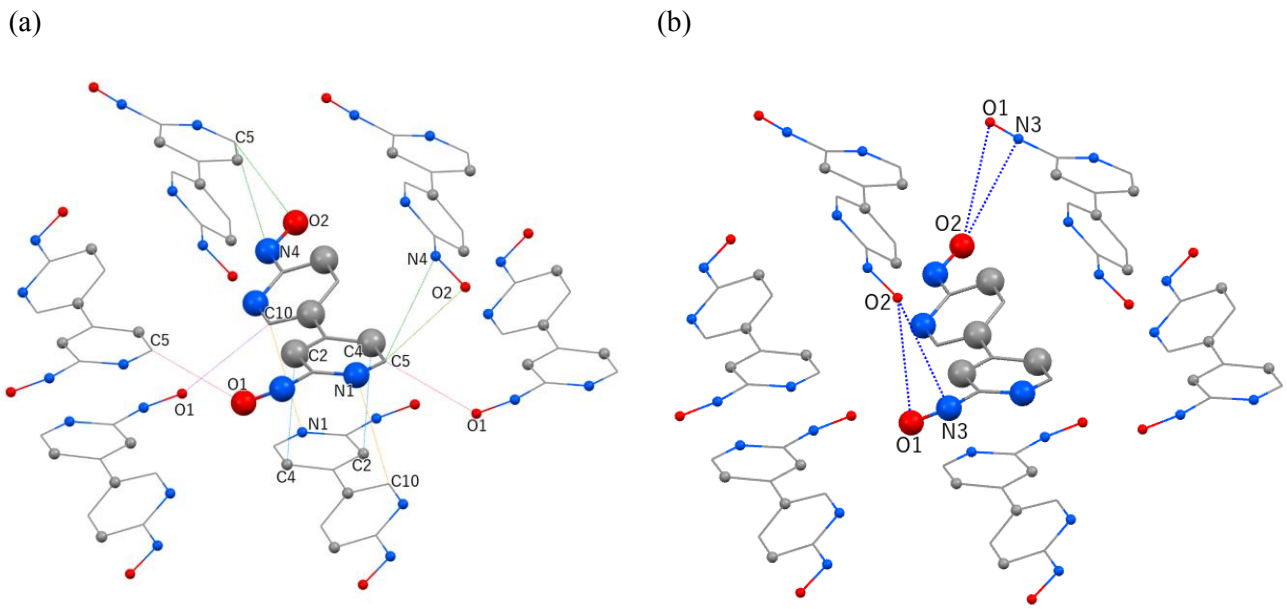

Figure S11 Crystal packing to show (a) all of the short intermolecular contacts (< 3.5 Å) and (b) the nearest neighbor nitroxide pairs in 34bpybNO. Each dotted line represents a distance between respective atoms of the centered molecule and other ones (see Table S1 for the distances). Spheres on molecules emphasize atoms with a large spin density (e.g., O1, O2, N3, N4, C2, C4, according to spin density surfaces in Fig. S7). Hydrogen atoms and *tert*-butyl groups are omitted for clarity.

Table S1 Intermolecular exchange couplings estimated by DFT calculations

Contacts d / Å	Spin density surfaces[a]	E_T / a.u. $\langle S^2 \rangle_T$	E_{BS} / a.u. $\langle S^2 \rangle_{BS}$	$2j\ k_B^{-1}$ / K
O2···O1 3.660(2) O2···N2 3.834(2)	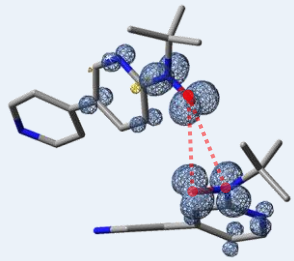	−1564.81818689 2.0002	−1564.81818438 0.1499	+0.86
O2···C5 3.273(3) N4···C5 3.470(3)	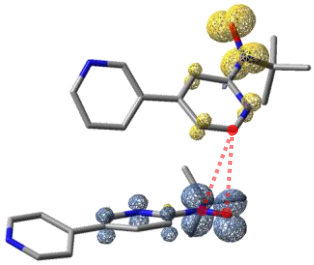	−1564.81686469 2.0002	−1564.81687143 0.1500	−2.30
O1···C5 3.143(3)	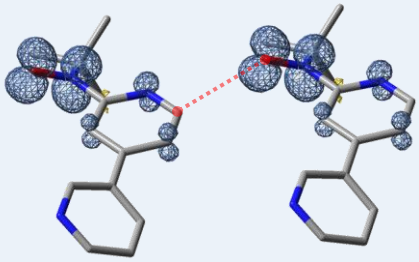	−1564.79678195 2.0002	−1564.79677553 0.1343	+2.17
O1···C10 3.469(3)	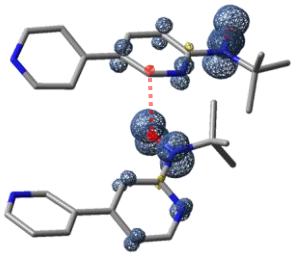	−1564.81962325 2.0002	−1564.81962238 0.1514	+0.30
N1···C10 3.374(3)	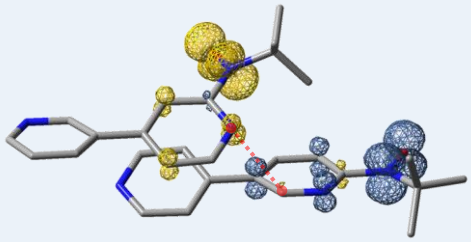	−1564.81369565 2.0002	−1564.81369766 0.1526	−0.69

[a] The isovalue is set to 0.007 e$^-$ a.u.$^{-3}$. Hydrogen atoms are omitted for clarity..

Magnetic analyses

We estimated exchange coupling parameters, J and j, for 34bpybNO in a crystalline solid state using a four-spin model[7] in consideration of a biradical dimer unit having a π–π interaction as a meaningful magnetic interaction path, which is defined by the spin Hamiltonian of $H = -2J(S_1 \cdot S_2 + S_3 \cdot S_4) - 2jS_2 \cdot S_3$. The g value was fixed as a constant of 2.0059 estimated from the ESR result. The curve fittings based on the least-squares method were performed to the χ_{mol} vs T plot. We tested curve fittings using corresponding χ_{mol} values in varied temperature ranges: 4.2–300, 5–300, 6–300, 7–300, 8–300 and 10–300 K. The resultant parameters are listed in Table S2. The parameters of J, j and θ were estimated as the average values among Results 2–5 which well reproduce the experimental χ_{mol} data, being in good agreement with those of the DFT calculations (see above). The susceptibilities in such a temperature region mainly reflect the intramolecular and intradimer exchange couplings and are relatively free from influences of trivial paramagnetic impurities and residual weak intermolecular magnetic interactions which become noticeable below a Weiss temperature of θ = ~5 K. In addition, to check the validity of applying the four-spin model, we tried performing curve fittings by using a simple singlet–triplet model (taking account of only a biradical monomer unit) which is described as the Bleaney–Bowers equation. The best fit curves show in Fig. S12. No parameter satisfactorily reproducing the experimental data was obtained for the singlet–triplet model regardless of applying θ, where we found only two convergent results in the curve fittings using the singlet–triplet model with θ and they apparently deviate from the DFT results. Thus, we can conclude that the four-spin model is appropriate to the magnetic property of 34bpybNO in the crystalline state.

Table S2 The parameters obtained from the curve fittings using χ_{mol} data in varied temperature ranges

Result	Temp. range / K	$2J\,k_B^{-1}$ / K	$2j\,k_B^{-1}$ / K	θ / K	R (= $[\Sigma(\chi_{obs}-\chi_{calc})^2/\Sigma\chi_{obs}^2]^{1/2}$)[a]
1	4.2–300	+73(3)	–69.7(18)	–7.1(3)	0.00376
2	5–300	+91(2)	–79.2(14)	–5.2(3)	0.00230
3	6–300	+106(3)	–85.6(14)	–4.0(2)	0.00308
4	7–300	+111(4)	–87.6(17)	–3.6(3)	0.00366
5	8–300	+98(5)	–83(2)	–4.5(4)	0.00248
6	10–300	+79(3)	–77.9(13)	–5.5(3)	0.00584
average[b]		**+101(10)**	**–84(5)**	**–4.4(8)**	

[a] Residual factor for observed and calculated values of magnetic susceptibilities.

[b] Averaged values were obtained using the parameters estimated for Results 2–5.

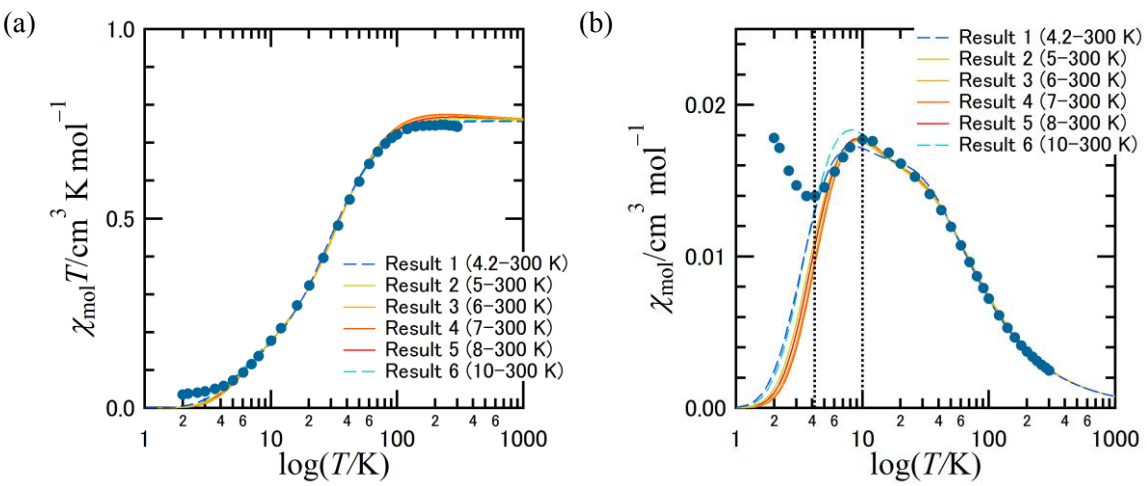

Figure S12 Temperature dependences (logarithmic scale) of (a) $\chi_{mol}T$ and (b) χ_{mol} at 5 kOe for 34bpybNO in a crystalline solid state (circles). Solid and dashed lines stand for the best fit curves of a four-spin model using the experimental χ_{mol} data in the temperature ranges from 4.2 (blue), 5 (yellow), 6 (gold), 7 (orange), 8 (red), 10 (cyan) to 300 K. Dotted lines mark boundaries at 4.2 and 10 K.

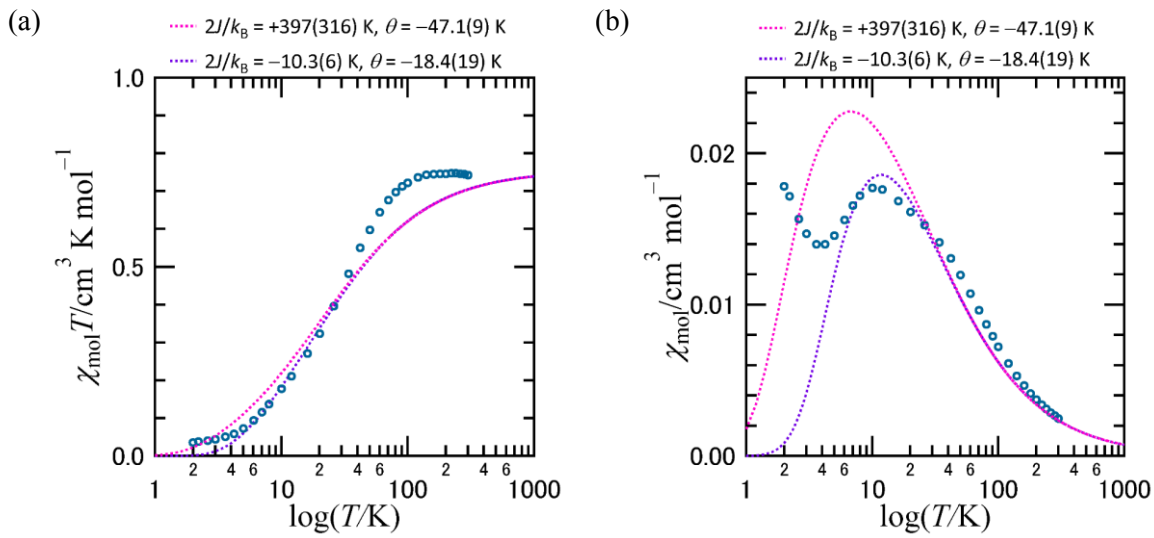

Figure S13 Temperature dependences (logarithmic scale) of (a) $\chi_{mol}T$ and (b) χ_{mol} at 5 kOe for 34bpybNO in a crystalline solid state (open circles) with the best fit curves of a singlet–triplet model described as Bleaney–Bowers equation containing a Weiss mean field parameter (θ). Two results were displayed, while any other convergent parameters were never obtained for the singlet–triplet model.

ESR and UV–vis spectra

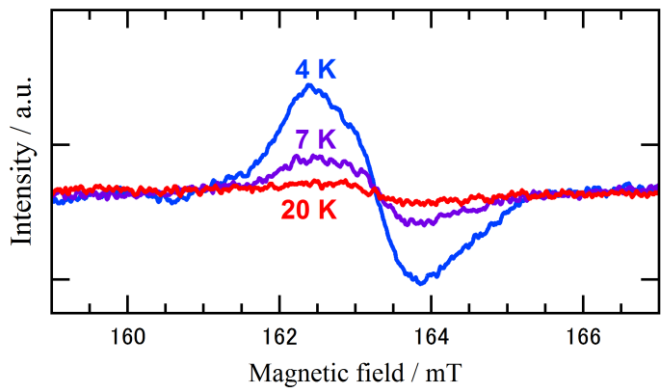

Figure S14 Temperature dependence of $|\Delta m_S| = 2$ (forbidden transition) band in X-band ESR spectra of 34bpybNO in a frozen toluene/methanol solution.

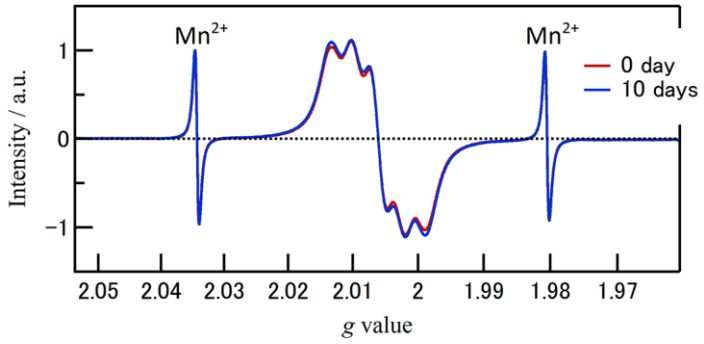

Figure S15 Time variation of ESR spectrum of 34bpybNO in toluene (1.0×10^{-4} M). The 'Mn^{2+}' labels denote the signals of a Mn^{2+} marker. No decomposition of the biradical was observed in 10 days within an experimental error of at most 5%.

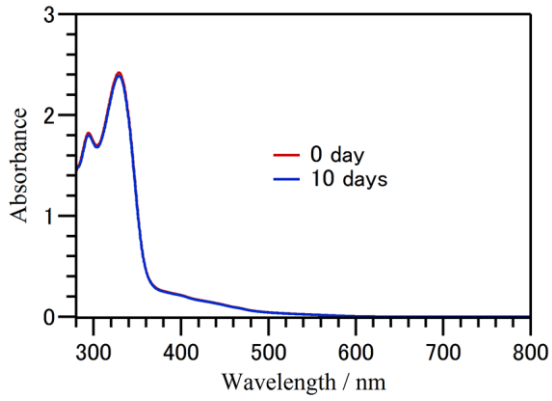

Figure S16 Time variation of UV–vis spectrum of 34bpybNO in toluene (1.0×10^{-4} M). No decomposition of the biradical was observed in 10 days within an experimental error of at most 5%.

References

1 A. S. Voisin-Chiret, A. Bouillon, G. Burzicki, M. Célant, R. Legay, H. El-Kashef, S. Rault, *Tetrahedron*, **2009**, *65*, 607.

2 M. J. Frisch, G. W. Trucks, H. B. Schlegel, G. E. Scuseria, M. A. Robb, J. R. Cheeseman, G. Scalmani, V. Barone, B. Mennucci, G. A. Petersson, H. Nakatsuji, M. Caricato, X. Li, H. P. Hratchian, A. F. Izmaylov, J. Bloino, G. Zheng, J. L. Sonnenberg, M. Hada, M. Ehara, K. Toyota, R. Fukuda, J. Hasegawa, M. Ishida, T. Nakajima, Y. Honda, O. Kitao, H. Nakai, T. Vreven, J. A. Montgomery, Jr., J. E. Peralta, F. Ogliaro, M. Bearpark, J. J. Heyd, E. Brothers, K. N. Kudin, V. N. Staroverov, R. Kobayashi, J. Normand, K. Raghavachari, A. Rendell, J. C. Burant, S. S. Iyengar, J. Tomasi, M. Cossi, N. Rega, J. M. Millam, M. Klene, J. E. Knox, J. B. Cross, V. Bakken, C. Adamo, J. Jaramillo, R. Gomperts, R. E. Stratmann, O. Yazyev, A. J. Austin, R. Cammi, C. Pomelli, J. W. Ochterski, R. L. Martin, K. Morokuma, V. G. Zakrzewski, G. A. Voth, P. Salvador, J. J. Dannenberg, S. Dapprich, A. D. Daniels, Ö. Farkas, J. B. Foresman, J. V. Ortiz, J. Cioslowski, D. J. Fox, *Gaussian 09 (Revision B.01)*, Gaussian, Inc., Wallingford CT, **2009**.

3 A. D. Becke, *J. Chem. Phys.* **1993**, *98*, 5648.

4 C. Lee, W. Yang, R. G. Parr, *Phys. Rev. B* **1998**, *37*, 785.

5 a) E. Ruiz, J. Cano, S. Alvarez, P. Alemany, *J. Comput. Chem.* **1999**, *20*, 1391. b) L. Noodleman, C. Y. Peng, D. A. Case, J. M. Mouesca, *Coord. Chem. Rev.* **1995**, *144*, 199.

6 M. Nishino, S. Yamanaka, Y. Yoshioka, K. Yamaguchi, *J. Phys. Chem. A* **1997**, *101*, 705.

7 a) J. W. Hall, W. E. Estes, E. D. Estes, R. P. Scaringe, W. E. Hatfield, *Inorg. Chem.*, **1977**, *16*, 1572. b) A. Okazawa, D. Hashizume, T. Ishida, *J. Am. Chem. Soc.*, **2010**, *132*, 11516.